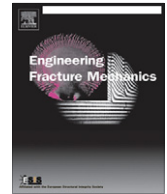




ELSEVIER

Contents lists available at SciVerse ScienceDirect

Engineering Fracture Mechanics

journal homepage: www.elsevier.com/locate/engfracmech

Punching shear resistance of concrete slabs using mode-II fracture energy

Ch. Naga Satish Kumar, T.D. Gunneswara Rao*

Department of Civil Engineering, National Institute of Technology, Warangal 506 004, India

ARTICLE INFO

Article history:

Received 31 March 2011

Received in revised form 6 January 2012

Accepted 9 January 2012

Keywords:

Punching shear

Mode-II fracture parameters

Double edge notched specimen

ABSTRACT

In this paper an analytical model is presented to predict the punching shear resistance of concrete slabs using fracture energy concept. The mode-II fracture parameters are obtained by conducting the experiments on double edge notched specimens. The model predicts the force displacements resistance during punching and the stress distribution along the cracked surface. Experimental investigation on punching shear resistance of concrete slabs is also reported to compare the model. The punching shear tests showed that the thickness of slab had a strong influence on the punching shear strength and also very good agreement between the predicted and experimental results.

© 2012 Elsevier Ltd. All rights reserved.

1. Introduction

The resistance to the transverse effects of concentrated forces acting on concrete slabs is an essential problem in design of column footings, flat slabs and bridge slabs. Punching shear is usually the governing failure mode for flat slabs. In the slab column connections, high shear stresses are developed around supporting columns, which can lead to abrupt punching shear failure. The problem with this failure mode is that it is brittle and catastrophic due to the inability of the concrete to support the large tensile stresses that develop. This failure occurs with the potential diagonal crack following the surface of a truncated cone around the column. So punching shear in concrete slabs is a serious problem in a structural system.

Most research on the punching shear strength of slabs has been concerned with the generation of experimental data on simply supported slabs and the development of empirical equations. Theoretical analysis of punching shear strength of concrete slabs have been proposed by various investigators Braestrup [1], Jiang and Shen [2], Alexander and Simmonds [3], Yankalesky and Leibowitz [4] and Theodorakopoulos and Swamy [5]. These theories do not consider the post fracture properties of concrete.

Concrete is a quasi-brittle material that exhibits softening behavior as a result of micro cracking that develops due to its low tensile strength. In the punching shear, failure occurs by slipping of a truncated cone around the column with the adjacent concrete layer. Therefore, it is assumed that the energy dissipated per unit area of cracked surface is equal to the fracture energy of concrete in mode-II. Several experimental and numerical tests were carried out to determine the mode-II fracture energy. Bazant and Pfeiffer [6] and Reinhardt and Xu [7] proposed for mode-II fracture energy values about 25 times greater than those of mode-I fracture energy. Gunneswara Rao and Naga Satish Kumar [8] have suggested method to assess the mode-II fracture energy using the size effect method based on the experiments on double edge notched specimens.

2. Research significance

Current methods for estimating the punching shear strength of concrete slabs rely on empirical formulation to estimate the contribution of concrete. This approach, in some cases, leads to very conservative estimates of punching shear strength of

* Corresponding author. Mobile: +91 9441136676.

E-mail address: tdgtg@gmail.com (T.D. Gunneswara Rao).

Nomenclature

τ_{\max}	maximum shear stress
Δ_{\max}	slip at the maximum shear stress
Δ_{cri}	critical slip
θ	the inclination of the sliding surface with vertical
σ	normal compressive stress
d_a	maximum aggregate size
d	column diameter
G_{IIIf}	mode-II fracture energy
D_s	support diameter of slab
P	punching resistance of slab
h	thickness of slab
MAS	maximum aggregate size

concrete slabs, but may also overestimate the contribution of concrete. In this paper a model for estimating the punching shear strength of concrete slabs based on the post-peak fracture properties of concrete is presented. The experimental results show that post fracture properties of concrete are necessary to understand the behavior of concrete slabs under concentrated loads. This work is expected to contribute for a better comprehension of the stress transfer mechanism along the cracked surface, particularly with respect to the qualitative and quantitative definition of mode-II fracture of concrete.

3. Analytical model

Consider a circular slab being connected to circular column which is subjected to an axial force (Fig. 1). The proposed model assumes that the shape of the sliding surface to be planar and the cracked surface is continuous and starts along the column circumference. The axial displacement μ , which is the relative displacement between the two rigid bodies of the slab and the column. The slip of the sliding surface is Δ , which is the tangential component of axial displacement. The crack width is 'w', which is the normal component of axial displacement. The rough crack surface geometry is responsible for dilation, or crack opening, accompanying shear displacement. When dilation is restrained to some extent, compressive stresses are developed normal to the cracked surface. Therefore two stress components are considered on the cracked surface i.e. shear stress (τ) and normal compressive stress (σ) (Fig. 1). The shear stress (τ) and normal compressive stress (σ) are assumed to be uniformly distributed along the planar inclined fracture surface. The tangential forces along the cracked surface contribute to an increase in the resistance and the compressive normal forces act to decrease the resistance.

A differential axi-symmetric surface area dA is

$$dA = \frac{2\pi r dy}{\cos \theta}$$

where 'r' is the radius of the sliding surface at a distance of 'y' from the top of the slab and θ is angle between the vertical and sliding surface

$$r = \frac{d}{2} + \frac{(D_s - d)y}{2h}$$

$$\tan \theta = \frac{D_s - d}{2h}$$

where 'd' is the column diameter, 'D_s' is the support diameter and 'h' is the thickness of slab.

The vertical component of shear resultant, acting on dA is

$$dP_{\tau} = \tau dA \cos \theta$$

The vertical force component resulting from the normal stress is

$$dP_{\sigma} = \sigma dA \sin \theta$$

Total punching resistance (P) = $\int (dP_{\tau} - dP_{\sigma})$

$$P = \int_0^h 2\pi(\tau - \sigma \tan \theta) r dy = 2\pi(\tau - \sigma \tan \theta) \left(\frac{hd}{2} + \frac{(D_s - d)h}{4} \right) \quad (1)$$

3.1. Shear stress and slip relationship

The shear stress and slip relationship established experimentally i.e. by performing a test on the double edge notched specimen of different grades of concrete with varying maximum aggregate size (MAS). The experimental results of double

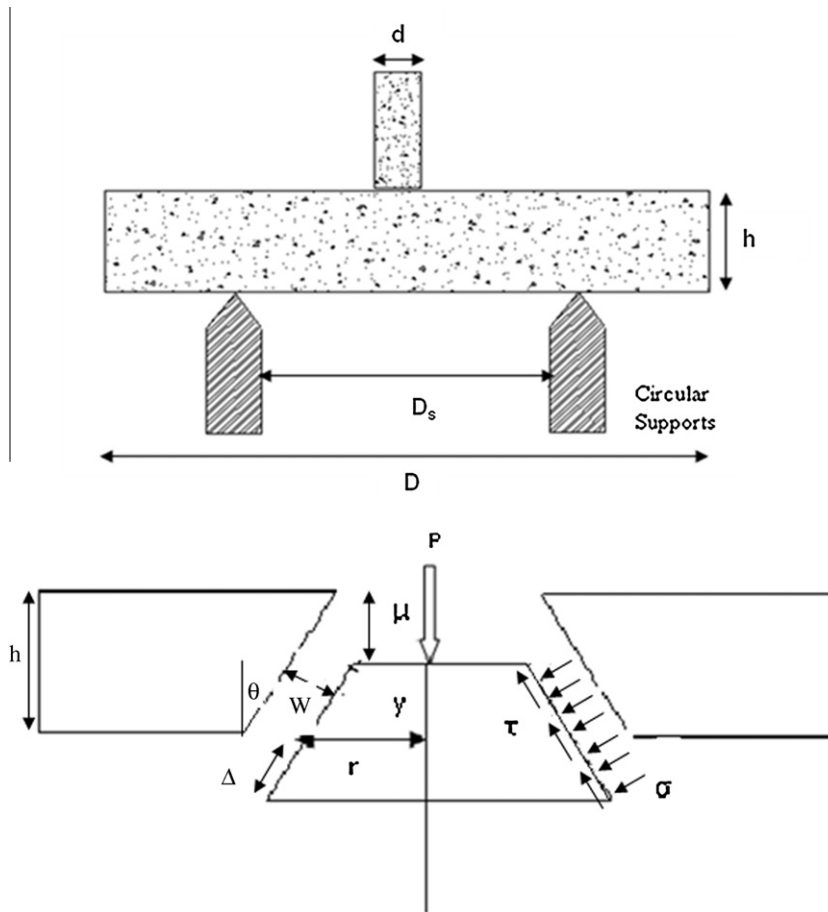


Fig. 1. Geometry of punching shear model.

edge notched specimen show that the specimen always fails in compression but before compression failure occurs, mode-II crack initiates. However closely after initiation mode-II crack growth is arrested and critical diagonal shear failure in compression is initiated. Finally, the compressive load at which the mode-II crack initiates is recorded. The fracture energy (G_{IIIF}) was calculated based on size effect method adopted by Gunneswara Rao and Naga Satish Kumar [8]. The maximum shear stress at the notch tip was calculated based on the numerical analysis carried out using finite element software (ANSYS). A Bakelite based 120-Ohm Electrical Resistance Strain Gauge (ERSG) with gauge factor 2.1 was used to measure strain of loaded portion and unloaded portion of the specimen (Fig. 2). The load strain diagram of loaded and unloaded portion of the double edge notched specimen ($f_{ck} = 23.5 \text{ N/mm}^2$ and $d_a = 20 \text{ mm}$) was presented in Fig. 3. The shear strain at maximum shear stress was determined by the relative difference of deformations in the loaded portion and unloaded portion of the specimen divided by the distance between the strain gauges. The slip is equal to the shear strain multiplied by three times the maximum aggregate size. In this investigation, the distance between strain gauges is taken as three times the maximum aggregate size based on the assumption that the length of the fracture process zone is three times the maximum aggregate size [9]. In this investigation, the relationship between the shear stress and slip with a linear softening branch was considered. This relationship was presented in Fig. 4. As indicated in this figure, the material parameters are: the maximum shear stress (τ_{max}), slip at the maximum shear stress (Δ_{max}), Critical slip i.e. slip at the zero shear stress (Δ_c), mode-II fracture energy (area under the shear stress and slip softening curve) these parameters were obtained from the experimental results. The details of compressive strength values, maximum aggregate size and mode-II fracture energy for the tested double edge notched specimens are shown in Table 1. From the experiments on double edge notched specimen of different grades of concrete (28 days Cube strength of concrete) with varying maximum aggregate size (MAS) the following formulas were obtained based on the regression analysis [10].

$$G_{IIIF} = 0.429d_a^{0.1461} f_{ck}^{0.3042} \quad (2)$$

$$\tau_{max} = 0.056 * f_{ck}^{1.171} \quad (3)$$



Fig. 2. Photograph of double edge notched specimen in the testing machine.

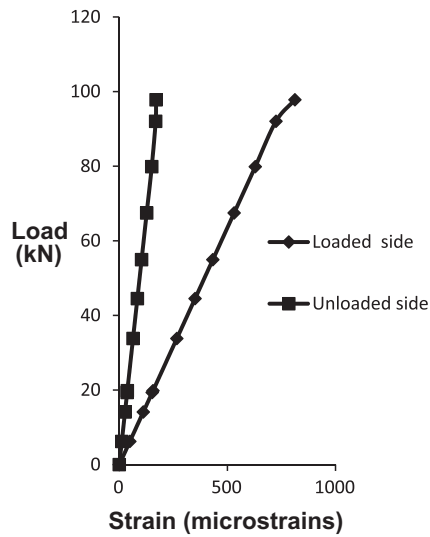


Fig. 3. Load–strain diagram of double edge notched specimen.

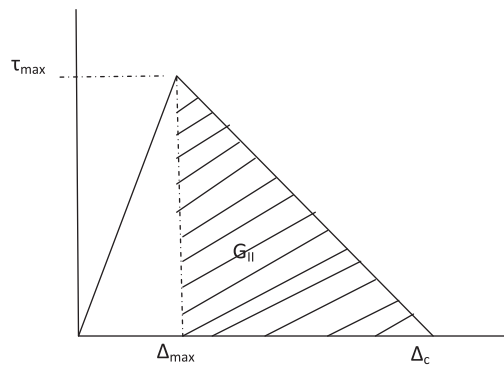


Fig. 4. Linear constitutive relationship between shear stress and slip.

$$\Delta_{\max} = (-2 \times 10^{-9} * f_{ck}^3 - 5 \times 10^{-8} * f_{ck}^2 + 9 \times 10^{-6} * f_{ck}) * 3d_a \tag{4}$$

$$\Delta_{\text{cri}} = \frac{2 * G_{II}}{\tau_{\max} + \Delta_{\max}} \tag{5}$$

Table 1

Details of compressive strength, maximum aggregate size and mode-II fracture energy for tested double edge notched specimens.

Compressive strength of concrete, f_{ck} (N/mm ²)	Maximum aggregate size, d_a (mm)	Fracture energy of concrete, G_{IIF} (N/mm)
23.5	20	1.727
21.2	16	1.640
20.5	10	1.461
38.23	20	2.033
37.2	16	1.968
36.8	10	1.886
59.2	20	2.308
58.5	16	2.180
56.2	10	2.003
82.5	20	2.505
81	16	2.482
79.2	10	2.271

where G_{IIF} is mode-II fracture energy in N/mm; τ_{max} is maximum shear stress in MPa, Δ_{max} is slip at the maximum shear stress, Δ_c is critical slip, f_{ck} is 28 days cube strength of concrete and d_a is maximum aggregate size.

3.2. Normal stress on a cracked surface

The relationship between shear stress and normal stress on an inclined plane before cracking and after cracking were obtained from the numerical analysis. The numerical analysis was performed using the finite element package i.e. ANSYS. The Solid 65 element was used to model the concrete (Fig. 5). The solid 65 element is a three-dimensional element, capable of cracking in tension and crushing in compression. The most important feature of this element is that it can represent both linear and non-linear behavior of the concrete. For the linear stage, the concrete is assumed to be an isotropic material up to cracking. For the non-linear part, the concrete may undergo plasticity [11]. Newton–Raphson equilibrium iteration was used for nonlinear analysis. A displacement controlled incremental loading was applied on the slab-column through the column. Small initial load steps were used for detecting first crack then automatic time stepping was used to control the load step sizes.

The main focus of this analysis is to study the variation of normal stress and shear stress with the angle ' θ ' (θ is the inclination of the sliding surface with vertical). A parametric study was carried out to look at the effect of shear stress and normal stress on different values of ' θ '. From the numerical analysis it was observed that the ratio of normal stress to shear stress in pre cracking stage increases when the inclination of sliding surface with respect to vertical increases (Fig. 6). But after cracking the ratio reduces to zero i.e. complete crack opening takes place and failure is by pure shear.

Using the above relations the model was developed for estimation of punching shear strength of concrete slabs, which has been implemented in a computer program which gets input of the geometry, material properties i.e. mode-II fracture energy (G_{IIF}), shear stress and shear strain. The stepwise procedure for obtaining the punching shear strength–displacement response of concrete slabs is as follows.

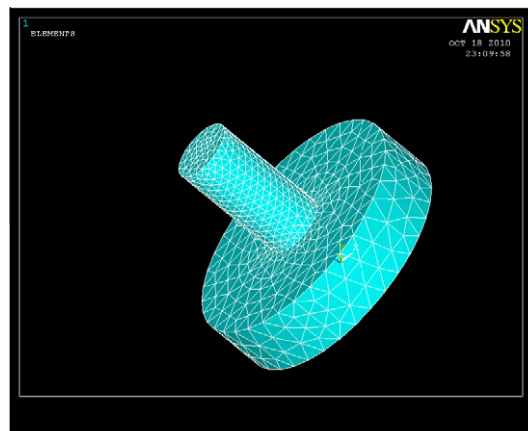


Fig. 5. ANSYS model for slab column specimen.

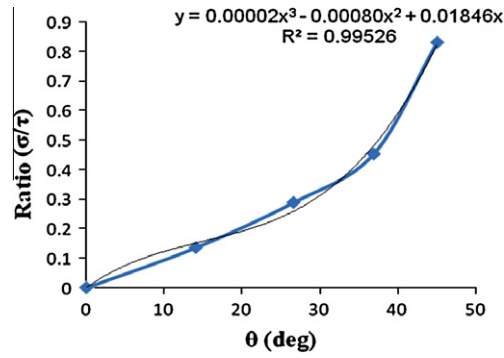


Fig. 6. Variation of normal stress to shear stress ratio with the inclination of sliding surface.

Step1: Determine the mode-II fracture energy (G_{II}) using the Eq. (2).

Step2: Determine the maximum shear stress (τ_{max}), maximum slip (Δ_{max}) and the critical slip (Δ_{cri}) using the Eqs. (3)–(5).

Step3: Calculate the slip (Δ) and crack width (w) of sliding surface of concrete for a given axial displacement (μ). $\Delta = \mu \cos \theta$; $w = \mu \sin \theta$.

Step4: Calculate the shear stress (τ) for slip (Δ) from the linear constitutive relationship between shear stress and slip. i.e.

$$\text{if } \Delta < \Delta_{max}; \quad \tau = \frac{\Delta * \tau_{max}}{\Delta_{max}},$$

$$\text{If } \Delta < \Delta_{cri} \text{ and } \Delta > \Delta_{max}; \quad \tau = \frac{(\Delta_{cri} - \Delta) * \tau_{max}}{(\Delta_{cri} - \Delta_{max})}.$$

Step5: Calculate the normal compressive stress σ using following equation:

$$\text{if } \Delta < \Delta_{max}; \quad \frac{\sigma}{\tau} = 0.00002 * \theta^3 - 0.0008 * \theta^2 + 0.0814 * \theta.$$

$$\text{If } \Delta > \Delta_{max}; \quad \frac{\sigma}{\tau} = 0.$$

Step 6: Calculate the Punching shear resistance for a given axial displacement μ using Eq. (1).

Step7: For complete punching shear strength–displacement response repeat the procedure from Step3 to Step6 giving suitable increment to axial displacement.

4. Experimental program

To validate the analytical model for estimating the punching resistance of concrete slab-column specimens were cast and tested. The experimental program consists of casting and testing two series of slab-column specimens without flexural reinforcement in the slabs, namely 'A' and 'B'. In each series there are three different sizes of the slab column specimens were used i.e. 50 mm × 50 mm × 200 ($d \times h \times D$), 100 mm × 100 mm × 400 mm and 200 mm × 200 mm × 800 mm such that to maintain the geometrical similarity of the slab column specimens. In this 'd' represents diameter of the column, 'h' represents thickness of the slab and 'D' represents the diameter of the slab.

4.1. Material details

Ordinary Portland cement (OPC) of 53 grade conforming to ASTM C150 Type1 with specific gravity of 3.15 was used in Concrete mix. Natural river sand with specific gravity 2.60 meeting the requirements of ASTM C-33 was used as fine aggregate in the entire investigation. Crushed coarse aggregate passing through 20 mm sieve and retained on 10mm sieve (60%) and retained on 4.75 mm (40%) with specific gravity 2.7 was used. The details of mix proportions are listed in Table 2.

Table 2
Quantities of materials.

Mix	Cement (kg/m ³)	Fine aggregate (kg/m ³)	Coarse aggregate (kg/m ³)	Water (l)
A	383.16	572.10	1161.53	191.58
B	450.00	429.72	1246.81	185.40

4.2. Casting

Cubes of 100 mm size were used to determine the compressive strength of concrete. Cylinders with 150 mm diameter and 300 mm length were used to determine the splitting tensile strength of concrete. Prisms of 100 mm × 100 mm ×

Table 3
Details of slab-column specimens.

Specimen designation	Size of the specimens $d \times h \times D$ (mm)	No. of samples
A1	50 × 50 × 200	3
A2	100 × 100 × 400	3
A3	200 × 200 × 800	3
B1	50 × 50 × 200	3
B2	100 × 100 × 400	3
B3	200 × 200 × 800	3



Fig. 7. Photograph of slab column specimen in the testing machine.

Table 4
Mechanical properties of concrete.

Mix	Cube compressive strength (N/mm ²)	Split tensile strength (N/mm ²)	Modulus of rupture (N/mm ²)
A	26.74	2.76	3.25
B	48.10	3.42	4.55

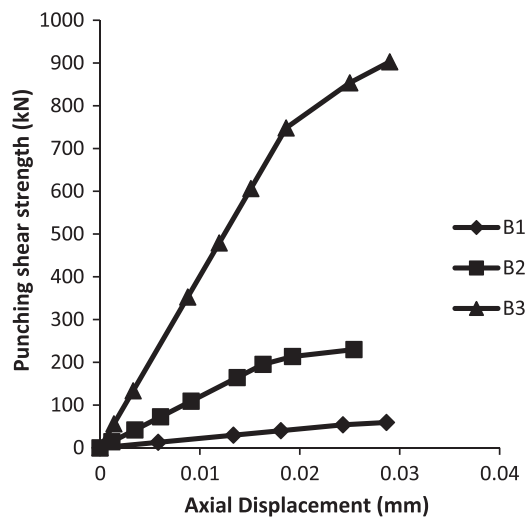


Fig. 8. Punching shear strength–displacement response of concrete slab up to the peak load of B-Series Specimens.

400 mm size were adopted to determine the modulus of rupture. Specially prepared steel molds were used for casting the slab column specimens. A needle and pan vibrator was used for compaction. All the specimens were water cured for 28 days. The specimen sizes used in the present study are shown in Table 3. In this experimental investigation a total of eighteen slab column specimens were cast and tested.

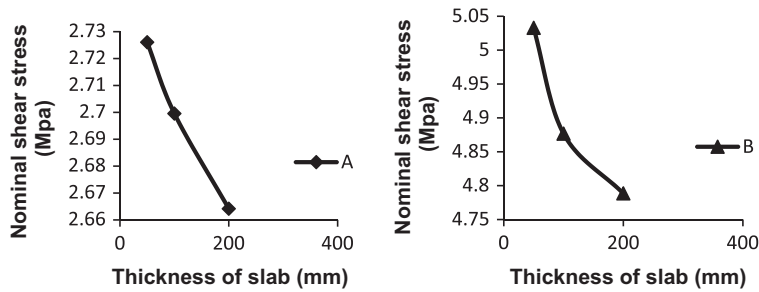


Fig. 9. Variation of nominal shear stress with the thickness of the slab.

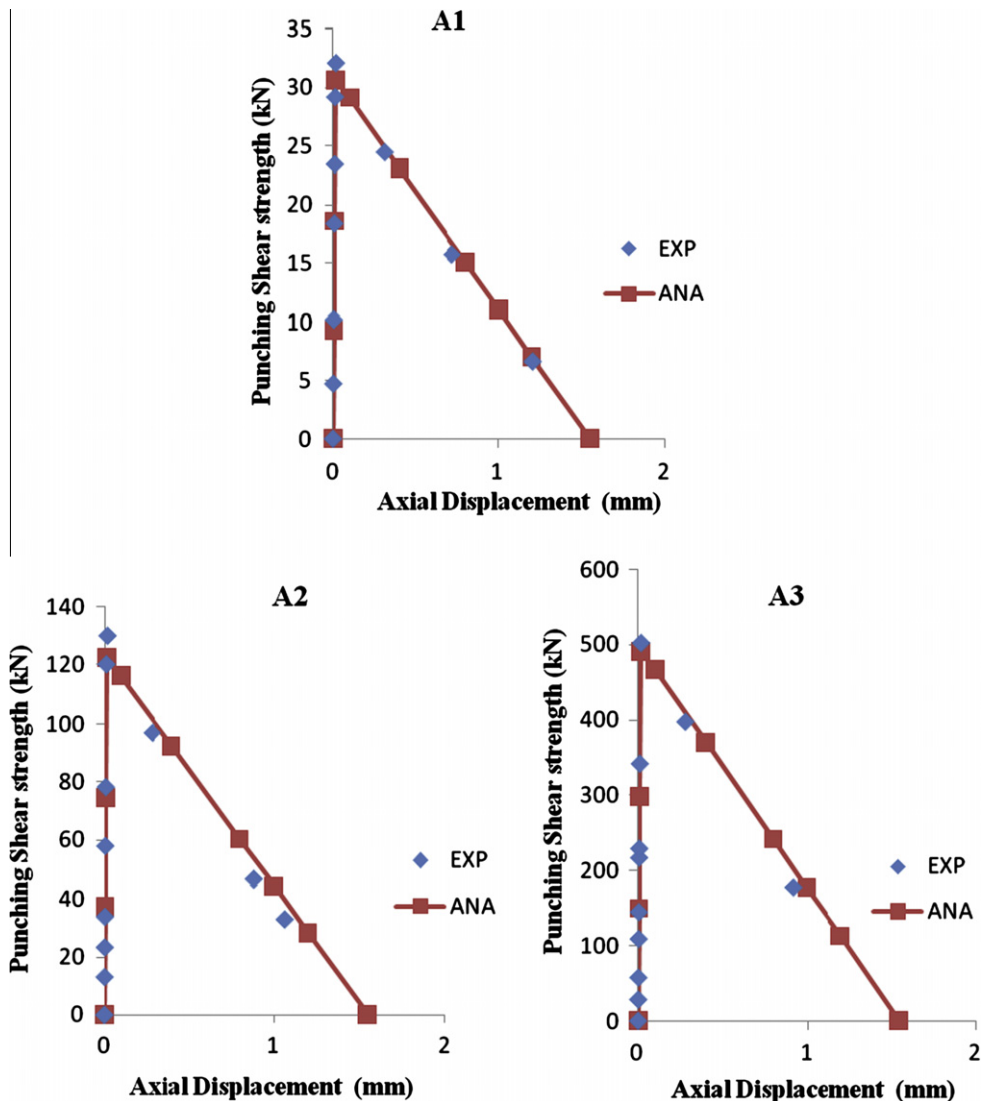


Fig. 10. Punching shear strength–displacement response of concrete slab-column A series.

4.3. Test setup and testing procedure

All the specimens were tested on the servo controlled dynamic testing machine of 1000 kN capacity under displacement control at a rate of 0.15 mm/min. The slab column specimen was kept at the center of testing machine and the specimen was placed on the specially prepared perimeter support consisted of a smooth continuous steel plate bent into a circular shape. The support diameter is 0.5 times the diameter of slab so that punching shear failure occurs. A photograph of the test setup is shown in Fig. 7. To find out the mechanical properties of concrete, three companion cubes, three companion cylinders and three companion prisms were cast from each batch and tested on the TOTM (Tinius Olsen testing machine of 400,000 lbs capacity). The average values of the mechanical properties of concrete are listed in Table 4.

5. Test results and discussions

The slab column specimens were tested on the servo controlled dynamic testing machine under displacement rate control. The load deflection relation is linear until cracking of the slab occurs. The first crack occurred at the tension side of the slab under the loaded area, and propagated across the slab to the sides in the radial direction. The stiffness of the slab is reduced upon the cracking and the load picks up again after the crack development has stabilized. There is a sudden drop in the load carrying capacity when the ultimate load is reached and the slab fails in punching shear. The load at which punching

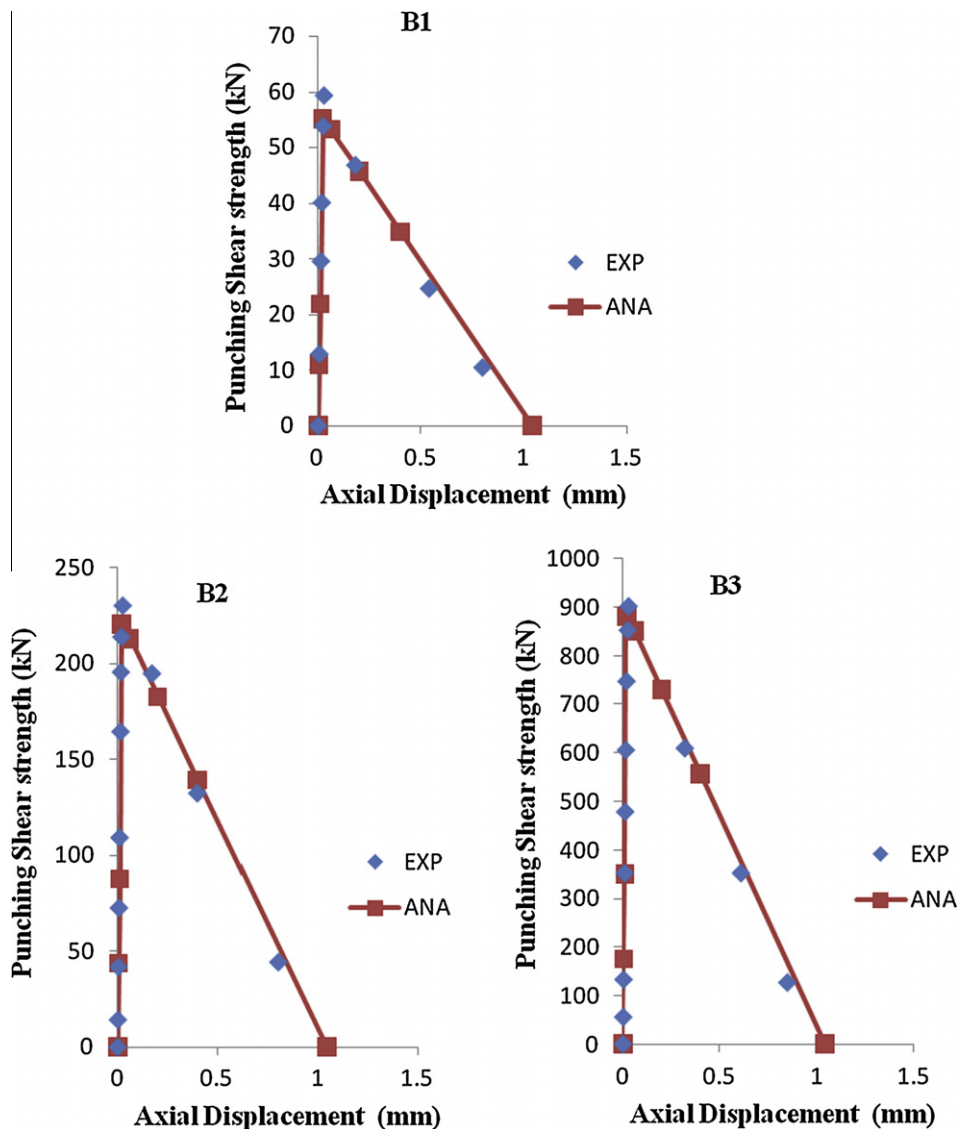


Fig. 11. Punching shear strength–displacement response of concrete slab-column B series.



Fig. 12. Photograph of specimens after the test.

Table 5
Comparison of test data with the model.

Specimen designation	Punching shear strength (kN)		Ratio P_{exp}/P_{ana}
	Experimental (P_{exp})	Model (P_{ana})	
A1	32.12	30.67	1.04
A2	130.12	122.70	1.06
A3	502.25	490.8	1.02
B1	59.30	55.19	1.07
B2	229.84	220.79	1.04
B3	902.74	883.55	1.02

shear failure occurred is recorded. Fig. 8 shows the punching shear strength–displacement response of concrete slab up to the peak load of B-Series Specimens. The variation of nominal shear stress with the thickness of the slab is presented in Fig. 9. From the Fig. 9, it is clear that the failure shear stress decreases with increasing the thickness of slab that indicates the punching shear strength of concrete slabs is strongly influenced by the thickness of slab. To understand the punching shear failure of concrete, load–displacement diagrams were drawn and presented in Figs. 10 and 11. These load–displacement diagrams exhibit a sharp peak followed by gradual softening. This confirms that the failure is caused by quasi-brittle cracking of concrete. A photograph of the tested samples is shown in Fig. 12.

The proposed model was used to predict the punching shear strength of plain concrete slabs i.e. without flexural reinforcement in the slabs and compared with the experimental data. The comparison of experimental results with analytical results was presented in Table 5. The ratio of experimental punching shear strength to the analytical punching shear strength is between 1.02 and 1.07. The results indicate that there exists a very good correlation between experimental and analytical values. This study reveals that the proposed analytical model can reasonably assess the punching shear strength–displacement response of concrete slabs.

6. Conclusions

Based on the analytical model and experimental work, the following conclusions have been drawn:

- (1) The proposed analytical model estimates the punching shear strength of concrete slabs satisfactorily.
- (2) Consideration of fracture properties of concrete i.e. mode-II fracture energy of concrete and slip of concrete at which complete shear failure occurs are essential for the punching shear strength–displacement response of concrete slabs.
- (3) From the experimental and analytical results, it was observed that the larger the slab thickness, the steeper the ascending curve of the punching shear strength–displacement curve. This confirms that the failure is caused by quasi-brittle cracking of concrete.
- (4) The punching shear strength of concrete slabs is strongly influenced by the thickness of slab.

Acknowledgements

The authors are very thankful to the authorities of National Institute of Technology, Warangal, for providing facilities for carrying out this work.

References

- [1] Braestrup MW. Punching shear in concrete slabs. Introductory report, IABSE Colloquium, Plasticity in reinforced concrete, Copenhagen, Denmark; 1987. p. 115–36.
- [2] Jiang Da-Hua, Shen Jing-Hua. Strength of concrete slabs in punching shear. *ASCE J Struct Engng* 1986;112(12):2578–91.
- [3] Alexander SDB, Simmonds SH. Ultimate strength of slab column connections. *ACI Struct J* 1987;255–61.
- [4] Yankelesky David A, Leibowitz Orit. Punching shear in concrete slabs. *Int J Mech Sci* 1999;41:1–15.
- [5] Theodorakopoulos DD, Swamy RN. Ultimate punching shear strength analysis of slab column connections. *Cement Concrete Compos* 2002;24:509–21.
- [6] Bazant ZP, Pfeiffer PA. Shear fracture tests of concrete. *Mater Struct* 1986;19:111–21.
- [7] Reinhardt Hans W, Xu Shilang. A practical testing approach to determine mode II fracture energy G_{IIF} for concrete. *Int J Fract* 2000;105:107–25.
- [8] Naga Satish Kumar Ch, Gunneswara Rao TD. Fracture parameters of high strength Concrete-mode-II testing. *Mag Concrete Res* 2010;62(3):157–62.
- [9] Bazant ZP, Oh BH. Crack band theory for fracture of concrete. *Mater Struct* 1983;16:155–77.
- [10] Ch Naga Satish Kumar. Mode-II fracture of concrete members: Application in Torsion and Punching shear. Ph.D. thesis submitted, NIT Warangal, Feb-2011.
- [11] Kheyroddin A, Hoseini vaez SR, Naderpour H. Numerical analysis of slab column connections strengthened with carbon fiber reinforced polymers. *J Appl Sci* 2008;8(3):420–31.